Palladium(II) and Platinum(II) Analogues of Luminescent Diimine *Triangulo* Complexes Supported by Triply Bridging Sulfide Ligands: Structural and Spectroscopic Comparisons

Biing-Chiau Tzeng,‡ Siu-Chung Chan, Michael C. W. Chan, Chi-Ming Che,* Kung-Kai Cheung, and Shie-Ming Peng†

Department of Chemistry, The University of Hong Kong, Pokfulam Road, Hong Kong SAR, China, and Department of Chemistry, National Taiwan University, Taipei, Taiwan

Received August 23, 2001

Reaction of $[M(L-L)Cl_2]$ [M = Pd, Pt; L−L = 4,4′-di-*tert*-butyl-2,2′-bipyridine ($^tBu_2$bpy), 4,4′-dimethylcarboxylate-2,2′-bipyridine ($(CO_2Me)_2$bpy), bis(diphenylphosphino)methane (dppm)] with Na_2S in refluxing methanol afforded $[M_3(^tBu_2bpy)_3(\mu_3\text{-}S)_2]^{2+}$ [M = Pd (**1a**), Pt (**2a**)], $[M_3((CO_2Me)_2bpy)_3(\mu_3\text{-}S)_2]^{2+}$ [M = Pd (**1b**), Pt (**2b**)], and $[Pt_3(dppm)_3(\mu_3\text{-}S)_2]^{2+}$ (**3**) as perchlorate salts. X-ray crystal analysis revealed that **1a**, **1b**, **2a**, and **3** have triangular M_3S_2 core structures. The three metal atoms in **1a**, **2a**, and **3** form virtual equilateral triangles with intramolecular Pd−Pd and Pt−Pt separations of 3.027(1)−3.065(1) and 3.104(1)−3.154(1) Å, respectively. An isosceles triangle of Pd_3 atoms is observed in the molecular structure of **1b**. The ^{1}MLCT absorption of **2a** and **2b** appears at 415 and 448 nm, respectively, in dichloromethane and is significantly red-shifted from the lowest energy absorption band of the Pd_3 analogues. Complex **1a** exhibits weak photoluminescence in the solid state at 77 and 298 K (uncorrected λ_{max} 760 and 730 nm, respectively) while the 77 K solid-state emission of **1b** (uncorrected λ_{max} 760 nm) is also weak. At 77 K, complexes **2a**, **2b**, and **3** display broad unstructured emissions at λ_{max} 616−630 nm in the solid state. Ligand-field excited states are tentatively assigned for these emissions.

Introduction

There has been considerable interest in the study of multinuclear d^8 metal complexes with bridging sulfide ligands.[1] This class of compounds displays diverse structural features and in some instances exhibits interesting reactivities and photoluminescence.[2,3] For example, the application of a series of $[Pt_2L_4(\mu_2\text{-}S)_2]$ (L = phosphine) metalloligands toward the construction of homo- and heteronuclear aggregates and clusters with the generic $[Pt_2M(\mu_3\text{-}S)_2]$ core has proved particularly fruitful.[2h] Indeed, phosphine ancillary ligands are chosen in the vast majority of cases, and there is a great paucity of trinuclear $[M_3S_2]$ derivatives bearing nitrogen donor ligands.[4] 2,2′-Bipyridines are attractive ligands for photochemical studies owing to their high absorbance in the UV region. As part of our ongoing investigation into the photophysics and photochemistry of luminescent polynuclear d^8 complexes, we have demonstrated that aromatic diimine and related cyclometalating ligands (e.g., 6-phenyl-2,2′-bipyridine) can impart beneficial emissive properties onto these systems.[5] We now describe the first examples of *triangulo* palladium(II) and platinum(II) complexes containing substituted 2,2′-bipyridine and triply bridging sulfide ligands, namely $[M_3(diimine)_3(\mu_3\text{-}S)_2][ClO_4]_2$ [M = Pd, Pt; diimine = 4,4′-di-*tert*-butyl-2,2′-bipyridine ($^tBu_2$bpy), 4,4′-dimethylcarboxylate-2,2′-bipyridine ($(CO_2Me)_2$bpy)], and examine their structural and luminescent characteristics. Moreover, the photophysical properties of the diphosphine congener $[Pt_3(dppm)_3(\mu_3\text{-}S)_2][ClO_4]_2$ is investigated and discussions on excited-state assignments are presented.

Experimental Section

General Procedures. K_2PdCl_4, K_2PtCl_4 (Strem), bis(diphenylphosphino)methane (dppm) (Lancaster), and Na_2S (Aldrich) were used as received. 4,4′-Di-*tert*-butyl-2,2′-bipyridine,[6a] 4,4′-dimethylcarboxylate-2,2′-bipyridine,[6b] and $Pt(dppm)Cl_2$[7] were prepared according to literature methods. All reactions were performed under a nitrogen atmosphere, and solvents for syntheses (analytical grade) were used without further purification. (**Caution!** *Perchlorate salts are potentially explosive and should be handled with care and in small amounts.*) Electrospray mass

* Corresponding author. Fax: +852 2857 1586. E-mail: cmche@hku.hk.
‡ Present Address: Department of Chemistry, National Chung Cheng University, 160 San-Hsing, Min-Hsiung, Chia-Yi, Taiwan 621.
† National Taiwan University.

(1) Dance, I.; Fisher, K. *Prog. Inorg. Chem*. **1994**, *41*, 637.
(2) (a) Chatt, J.; Mingos, D. M. P. *J. Chem. Soc. A* **1970**, 1243. (b) Werner, H.; Bertleff, W.; Schubert, U. *Inorg. Chim. Acta* **1980**, *43*, 199. (c) Cecconi, F.; Ghilardi, C. A.; Midollini, S. *Inorg. Chem*. **1983**, *22*, 3802. (d) Cowan, R. L.; Pourreau, D. B.; Rheingold, A. L.; Geib, S. J.; Trogler, W. C. *Inorg. Chem*. **1987**, *26*, 259. (e) Matsumoto, K.; Saiga, N.; Tanaka, S.; Ooi, S. *J. Chem. Soc., Dalton Trans*. **1991**, 1265. (f) Pilkington, M. J.; Slawin, A. M. Z.; Williams, D. J.; Woollins, J. D. *J. Chem. Soc., Dalton Trans*. **1992**, 2425. (g) Liu, H.; Tan, A. L.; Mok, K. F.; Mak, T. C. W.; Batsanov, A. S.; Howard, J. A. K.; Hor, T. S. A. *J. Am. Chem. Soc*. **1997**, *119*, 11006. (h) Fong, S. W. A.; Hor, T. S. A. *J. Chem. Soc., Dalton Trans*. **1999**, 639. (i) Tarlton, S. V.; Choi, N.; McPartlin, M.; Mingos, D. M. P.; Vilar, R. *J. Chem. Soc., Dalton Trans.* **1999**, 653. (j) Hidai, M.; Kuwata, S.; Mizobe, Y. *Acc. Chem. Res*. **2000**, *33*, 46. (k) Fong, S. W. A.; Yap, W. T.; Vittal, J. J.; Hor, T. S. A.; Henderson, W.; Oliver, A. G.; Rickard, C. E. F. *J. Chem. Soc., Dalton Trans*. **2001**, 1986.
(3) (a) Yam, V. W. W.; Yeung, P. K. Y.; Cheung, K. K. *Chem. Commun*. **1995**, 267. (b) Yam, V. W. W.; Yeung, P. K. Y.; Cheung, K. K. *Angew. Chem., Int. Ed. Engl.* **1996**, *35*, 739.
(4) Lowe, G.; Ross, S. A.; Probert, M.; Cowley, A. *Chem. Commun*. **2001**, 1288.
(5) Recent examples: (a) Wu, L. Z.; Cheung, T. C.; Che, C. M.; Cheung, K. K.; Lam, M. H. W. *Chem. Commun.* **1998**, 1127. (b) Lai, S. W.; Chan, M. C. W.; Cheung, T. C.; Peng, S. M.; Che, C. M. *Inorg. Chem.* **1999**, *38*, 4046. (c) Lai, S. W.; Cheung, T. C.; Chan, M. C. W.; Cheung, K. K.; Peng, S. M.; Che, C. M. *Inorg. Chem*. **2000**, *39*, 255. (d) Lu, W.; Chan, M. C. W.; Cheung, K. K.; Che, C. M. *Organometallics* **2001**, *20*, 2477. (e) Chan, S. C.; Chan, M. C. W.; Che, C. M.; Wang, Y.; Cheung, K. K.; Zhu, N. *Chem. Eur. J*. **2001**, *7*, 4180.
(6) (a) Bager, G. M.; Sasse, W. H. F. *J. Chem. Soc*. **1956**, 616. (b) Kocian, O.; Mortimer, R. J.; Beer, P. D. *Tetrahedron Lett*. **1990**, *31*, 5069.
(7) Slack, D. A.; Baird, M. C. *Inorg. Chim. Acta* **1977**, *24*, 277.

10.1021/ic010891r CCC: $20.00
Published on Web 11/10/2001

Table 1. Crystal Data

	1a$(ClO_4)_2\cdot H_2O$	**1b**$(ClO_4)_2\cdot H_2O$	**2a**$(ClO_4)_2\cdot H_2O$
formula	$C_{54}H_{74}N_6O_9Cl_2Pd_3S_2$	$C_{42}H_{38}N_6O_{21}Cl_2Pd_3S_2$	$C_{54}H_{74}N_6O_9Cl_2Pt_3S_2$
fw	1405.50	1417.02	1671.51
crystal system	orthorhombic	triclinic[a]	orthorhombic
space group	Pbcn	$P\bar{1}$ (no. 2)	Pbcn
crystal size, mm	0.10 × 0.20 × 0.50	0.30 × 0.15 × 0.10	0.15 × 0.15 × 0.30
a, Å	13.151(2)	16.742(2)	13.152(4)
b, Å	23.679(2)	18.250(3)	23.619(3)
c, Å	19.706(2)	20.189(3)	19.662(4)
V, Å^3	6137(1)	5890(1)	6107(1)
Z	4	4	4
D_c, g cm^{-3}	1.521	1.598	1.818
μ, cm^{-1}	10.66	11.42	70.39
F(000)	2853	2816	3248
$2\theta_{max}$, deg	50	51	50
R, R_w[b]	0.044, 0.045	0.062, 0.101	0.031, 0.037
residual ρ, e Å^{-3}	−0.45, +0.67	−0.94, +1.48	−0.51, +1.21

[a] $\alpha = 74.65(2)°$, $\beta = 87.65(2)°$, $\gamma = 81.97(2)°$. [b] $R = \sum||F_o| - |F_c||/\sum|F_o|$; $R_w = [\sum w(|F_o| - |F_c|)^2/\sum w|F_o|^2]^{1/2}$.

spectra were collected on a Finnigan MAT-95 LCQ mass spectrometer using samples dissolved in dichloromethane for injection. Positive ion FAB mass spectra were recorded on a Finnigan MAT95 mass spectrometer. Further details of instrumentation, solvent treatment for photophysical studies, and emission measurements have been given previously.[5b]

Syntheses. [M(tBu$_2$bpy)Cl$_2$] (M = Pd, Pt). [M(tBu$_2$bpy)Cl$_2$] were prepared by adopting literature methods.[8] In a typical reaction to synthesize [Pd(tBu$_2$bpy)Cl$_2$], a mixture of tBu$_2$bpy, K_2PdCl_4 (1 equiv), and 1 drop of concentrated HCl was heated in water until the aqueous phase became colorless (ca. 2 h). The yellow product was collected by filtration, washed with water, and dried under vacuum: ^{1}H NMR ($CDCl_3$): 9.26 (d, 2 H, J = 6.2 Hz, H(6)), 7.90 (d, 2 H, J = 1.9 Hz, H(3)), 7.51 (dd, 2 H, J = 6.2, 1.8 Hz, H(5)), 1.45 (s, 18 H, tBu).

[M((CO$_2$Me)$_2$bpy)Cl$_2$] (M = Pd, Pt). The above method was adopted except no HCl was added to prevent hydrolysis of ester groups. [Pd((CO$_2$Me)$_2$bpy)Cl$_2$] was isolated as a yellow-brown solid. Yield 86%. ^{1}H NMR ($CDCl_3$): 9.65 (d, 2 H, J = 5.9 Hz, H(6)), 8.66 (d, 2 H, J = 1.5 Hz, H(3)), 8.15 (dd, 2 H, J = 5.9, 1.7 Hz, H(5)), 4.11 (s, 6 H, MeO). [Pt((CO$_2$Me)$_2$bpy)Cl$_2$] was isolated as an orange solid. Yield: 85%.^{1}H NMR (DMSO-d_6): 9.71 (d, 2 H, J = 6.3 Hz, H(6)), 9.10 (d, 2 H, J = 1.6 Hz, H(3)), 8.25 (dd, 2 H, J = 6.1, 1.8 Hz, H(5)), 4.00 (s, 6 H, MeO).

[Pd$_3$(tBu$_2$bpy)$_3$(μ_3-S)$_2$][ClO$_4$]$_2$ (1a(ClO$_4$)$_2$). A mixture of Na_2S (0.16 g, 2.0 mmol) and [Pd(tBu$_2$bpy)Cl$_2$] (1.34 g, 3.0 mmol) in methanol (40 mL) was refluxed for 4 h. Upon cooling, the solution was filtered and the filtrate was concentrated to ca. 5 mL. Addition of excess $LiClO_4$ yielded a brown solid upon cooling at 0 °C for 12 h. Recrystallization of the crude product by diffusion of diethyl ether into an acetonitrile solution afforded yellow crystals. Yield: 0.72 g, 52%. Anal. Calcd for $C_{54}H_{72}N_6O_8Cl_2Pd_3S_2$: C, 46.75; H, 5.23; N, 6.06. Found: C, 46.57; H, 5.44; N, 5.78%. ES−MS: m/z = 594 [M]$^{2+}$, 1287 [M + ClO_4]$^+$. ^{1}H NMR ($CDCl_3$): 9.17 (d, 6 H, J = 5.9 Hz, H(6)), 7.91 (d, 6 H, J = 1.7 Hz, H(3)), 7.79 (dd, 6 H, J = 5.9, 1.9 Hz, H(5)), 1.41 (s, 54 H, tBu).

[Pt$_3$(tBu$_2$bpy)$_3$(μ_3-S)$_2$][ClO$_4$]$_2$ (2a(ClO$_4$)$_2$). The procedure for **1a** was adopted using Na_2S (0.16 g, 2.0 mmol) and [Pt(tBu$_2$bpy)Cl$_2$] (1.60 g, 3.0 mmol) to give the product as yellow crystals. Yield: 0.89 g, 54%. Anal. Calcd for $C_{54}H_{72}N_6O_8Cl_2Pt_3S_2$: C, 39.23; H, 4.39; N, 5.08. Found: C, 39.51; H, 4.44; N, 4.88%. ES−MS: m/z = 727 [M]$^{2+}$, 1553 [M + ClO_4]$^+$. ^{1}H NMR (CD_2Cl_2): 9.26 (d, 6 H, J = 6.1 Hz, H(6)), 8.03 (d, 6 H, J = 1.8 Hz, H(3)), 7.78 (dd, 6 H, J = 6.0, 1.9 Hz, H(5)), 1.47 (s, 54 H, tBu).

[Pd$_3$((CO$_2$Me)$_2$bpy)$_3$(μ_3-S)$_2$][ClO$_4$]$_2$ (1b(ClO$_4$)$_2$). The procedure for **1a** was adopted using Na_2S (0.04 g, 0.5 mmol) and [Pd((CO$_2$Me)$_2$bpy)Cl$_2$] (0.3 g, 0.67 mmol) to give the product as orange-brown crystals. Yield: 0.10 g, 32%. Anal. Calcd for $C_{42}H_{36}N_6O_{20}Cl_2Pd_3S_2$: C, 36.06; H, 2.59; N, 6.01. Found: C, 35.83; H, 2.55; N, 6.08%. ES−MS: m/z = 600 [M]$^{2+}$, 1299 [M + ClO_4]$^+$. ^{1}H NMR ($CDCl_3$): 9.59 (d, 6 H, J = 5.6 Hz, H(6)), 8.69 (d, 6 H, J = 1.2 Hz, H(3)), 8.38 (dd, 6 H, J = 5.6, 1.6 Hz, H(5)), 4.06 (s, 18 H, MeO).

[Pt$_3$((CO$_2$Me)$_2$bpy)$_3$(μ_3-S)$_2$][ClO$_4$]$_2$ (2b(ClO$_4$)$_2$). A mixture of Na_2S (53 mg, 0.67 mmol) and [Pt((CO$_2$Me)$_2$bpy)Cl$_2$] (0.54 g, 1.0 mmol) in methanol (50 mL) was refluxed under nitrogen for 4 h. Upon cooling, the solution was filtered and the filtrate was evaporated to dryness. Deionized water (20 mL) was added to dissolve the black residue. Addition of excess $LiClO_4$ to the filtrate yielded a brown solid. Dissolution of the crude product in acetonitrile (15 mL) and addition of diethyl ether (12 mL) afforded a black precipitate which was removed by filtration. Volatile components were removed from the resultant yellow filtrate to give an orange solid. Yield: 22 mg, 4%. Anal. Calcd for $C_{42}H_{36}N_6O_{20}Cl_2Pt_3S_2\cdot 3H_2O$: C, 29.34; H, 2.46; N, 4.89. Found: C, 29.57; H, 2.10; N, 4.49%. ES−MS: m/z = 733 [M]$^{2+}$, 1565 [M + ClO_4]$^+$. ^{1}H NMR ($CDCl_3$): 9.93 (d, 6 H, J = 5.9 Hz, H(6)), 8.65 (d, 6 H, J = 1.6 Hz, H(3)), 8.40 (dd, 6 H, J = 5.8, 1.6 Hz, H(5)), 4.07 (s, 18 H, MeO).

[Pt$_3$(dppm)$_3$(μ_3-S)$_2$][ClO$_4$]$_2$ (3(ClO$_4$)$_2$). Complex **3** has been prepared previously as the tetraphenylborate salt,[9] but an alternative procedure was used in this work. A mixture of Na_2S (15 mg, 0.19 mmol) and [Pt(dppm)Cl$_2$] (0.18 g, 0.28 mmol) in methanol (20 mL) was refluxed for 4 h. Upon cooling, excess $LiClO_4$ was added and the mixture was stood for 12 h to yield a yellow solid. Recrystallization of the crude product from diffusion of diethyl ether into an acetonitrile solution afforded pale yellow crystals. Yield: 0.15 g, 81%. Anal. Calcd for $C_{75}H_{66}P_6O_8Cl_2Pt_3S_2\cdot CH_3CN$: C, 45.28; H, 3.4; N, 0.69. Found: C, 45.46; H, 3.65; N, 0.42%. MS (+ve FAB): m/z 1802 [M + ClO_4]$^+$. ^{1}H NMR (DMSO-d_6): 7.75 (m, 24 H, H(2)), 7.45 (br t, 12 H, H(4)), 7.20 (br t, 24 H, H(3)), 5.41 (br t, 6 H, CH_2).

X-ray Crystallography. Crystal data and details of collection and refinement for [**1a**$(ClO_4)_2\cdot H_2O$], [**1b**$(ClO_4)_2\cdot H_2O$], and [**2a**$(ClO_4)_2\cdot H_2O$] are summarized in Table 1. Full crystallographic data for **3**$(ClO_4)_2$ is provided in the Supporting Information. For [**1a**$(ClO_4)_2\cdot H_2O$], a total of 5386 unique reflections was collected at 298 K on a Enraf-Nonius CAD4 diffractometer [λ(Mo Kα) = 0.710 73 Å, $\theta/2\theta$ scans]. The structure was solved by Patterson methods, expanded using Fourier techniques, and refined by least-squares treatment on F^2 using the NRCVAX program for 2648 absorption-corrected (transmission 0.971−1.000) reflections with $I > 2\sigma(I)$ and 345 parameters. For [**1b**$(ClO_4)_2\cdot H_2O$], a total of 20 348 unique reflections was collected at 301 K on a MAR diffractometer with a 300 mm image plate detector [λ(Mo Kα) = 0.710 73 Å]. The structure was solved by Patterson methods, expanded using Fourier techniques (PATTY[10]), and refined by full-

(8) (a) Hodges, F. G.; Watson, H. R. *J. Chem. Soc.* **1958**, 2772. (b) Hodges, K. D.; Rund, J. V. *Inorg. Chem.* **1975**, *14*, 525.
(9) Matsumoto, K.; Takahashi, K.; Ikuzawa, M.; Kimoto, H. *Inorg. Chim. Acta* **1998**, *281*, 174.
(10) PATTY: Beurskens, P. T.; Admiraal, G.; Beursken, G.; Bosman, W. P.; Garcia-Granda, S.; Gould, R. O.; Smits, J. M. M.; Smykalla, C. *The DIRDIF program system*; Technical Report of the Crystallography Laboratory; University of Nijmegen, The Netherlands, 1992.

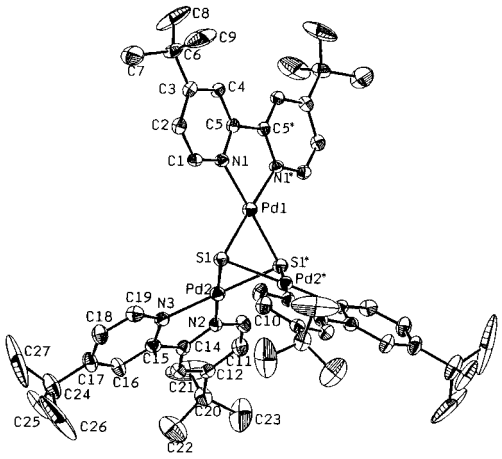

Figure 1. Perspective view of cation in **1a**$(ClO_4)_2 \cdot H_2O$ (40% probability ellipsoids).

matrix least squares on F using TeXsan[11] for 14 265 reflections with $I > 3\sigma(I)$ and 1279 parameters. A crystallographic asymmetric unit of [**1b**$(ClO_4)_2 \cdot H_2O$] consists of two molecular units. For [**2a**$(ClO_4)_2 \cdot H_2O$], a total of 5947 unique reflections was collected at 301 K on a Rigaku AFC7R diffractometer [λ(Mo Kα) = 0.710 73 Å, $\omega - 2\theta$ scans]. The structure was solved by Patterson methods, expanded using Fourier techniques (PATTY), and refined by full-matrix least squares using the TeXsan software package for 3099 absorption-corrected (transmission 0.742−1.000) reflections with $I > 3\sigma(I)$ and 344 parameters.

Results and Discussion

Synthesis and Characterization. Although transition metal complexes containing a M_3 triangle capped by two sulfide groups are in abundance in the literature, virtually all examples for group 10 are phosphine-ligated and there has been no reported precedent for such complexes containing aromatic α-diimine auxiliaries. In this work, $[M_3(diimine)_3(\mu_3\text{-}S)_2][ClO_4]_2$ [M = Pd, Pt] were prepared by treating [M(diimine)Cl_2] with Na_2S in refluxing methanol under a nitrogen atmosphere. This procedure afforded moderate yields (50−55%) for the ^{t}Bu$_2$bpy complexes. Due to the low solubility of the [M((CO$_2$Me)$_2$bpy)-Cl_2] precursors in the reaction mixture, low yields (~30%) were obtained for the Pd_3 derivative **1b** while the Pt_3 species **2b** was typically prepared in less than 5% yield. All characterization data are fully consistent with the proposed formulation for each complex. The phosphine-ligated $[Pt_3(dppm)_3(\mu_3\text{-}S)_2][ClO_4]_2$ (**3**$(ClO_4)_2$) derivative was obtained in good yield (81%) using this approach. The perchlorate salts of all complexes are stable in solid and solution states; no decomposition or ligand dissociation was observed in dichloromethane or acetonitrile. The electrospray mass spectra for dichloromethane solutions of the $[M_3(diimine)_3(\mu_3\text{-}S)_2]$ complexes **1a**,**b** and **2a**,**b** are dominated by an intense cluster of peaks assigned to the $[M_3(diimine)_3(\mu_3\text{-}S)_2(ClO_4)]^+$ ions. The remaining discernible cluster of signals (peaks separated by 0.5 amu) are attributed to the $[M_3(diimine)_3(\mu_3\text{-}S)_2]^{2+}$ species. We note that the bridging and capping abilities of the sulfide moiety, plus the propensity for Pd(II) and Pt(II) centers to aggregate, is intrinsic to the assembly of the *triangulo* $[M_3S_2]$ complexes.

Complexes **1a**, **1b**, **2a**, and **3** (see Supporting Information) have been structurally characterized by X-ray crystallography. Perspective drawings of the cations in **1a**, **1b**, and **2a** are shown in Figures 1, 2, and 3, respectively, while selected bond lengths and bond angles are listed in Table 2. The three complex cations

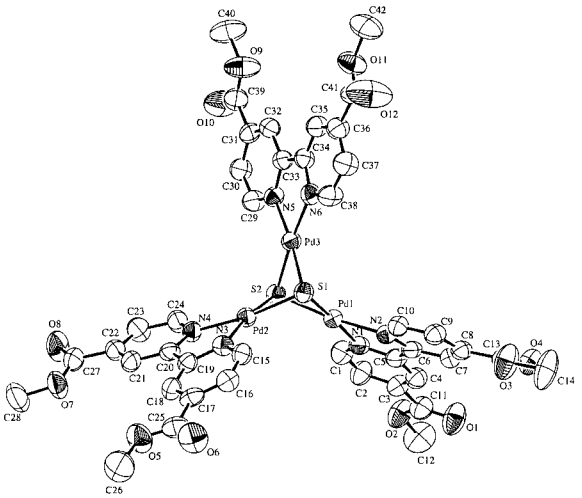

Figure 2. Perspective view of one of the two independent cations in **1b**$(ClO_4)_2 \cdot H_2O$ (30% probability ellipsoids).

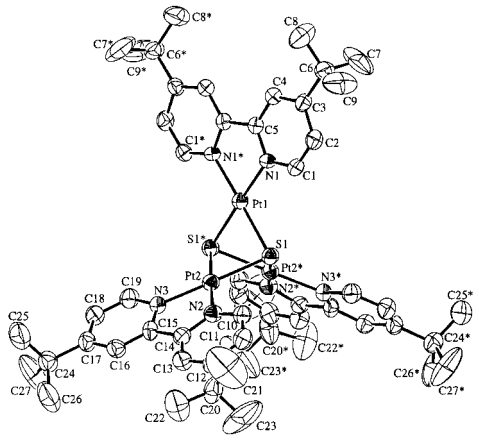

Figure 3. Perspective view of cation in **2a**$(ClO_4)_2 \cdot H_2O$ (40% probability ellipsoids).

are isostructural: each depicts three [M(α-diimine)] fragments capped by two triply bridging sulfur atoms, and M_3S_2 cores with distorted trigonal bipyramidal geometry are evident. The metal centers in the *cis*-[M(diimine)S_2] moieties reside in slightly distorted square-planar environments. For **1a**, **2a**, and **3**, the three metal nuclei virtually constitute an equilateral triangle. In contrast, the Pd_3 moiety in the two molecular units of **1b** form isosceles triangles. There is a crystallographic C_2 element passing through M(1) and the midpoint of the M(2)···M(2*) axis in **1a** and **2a**.

The metal−metal separations [3.027(1)−3.065(1) Å for **1a**, 3.127(1)−3.154(1) Å for **2a**, 3.013(1)−3.175(1) Å for **1b**, and 3.1040(9) Å for **3**] are outside the range expected for strong intermetal interactions, but are typical for corresponding phosphine-bound $[M_3S_2]$ derivatives[2,12] (3.00−3.18 Å for M = Pd, 3.11−3.18 Å for M = Pt) and open up the possibility for weak metal−metal interactions in these *triangulo* complexes. We note that the previous crystallographic reports of analogous P-donor derivatives have intriguingly described M_3 triangles of both equilateral (like **1a**, **2a**, and **3**) and isosceles (like **1b** with two edges long/one short or two edges short/one long) geometry for chemically very similar d^8 derivatives.[2,12] No rationale has

(11) TeXsan: *Crystal Structure Analysis Package*; Molecular Structure Corporation: The Woodlands, TX, 1985 and 1992.

(12) (a) Bushnell, G. W.; Dixon, K. R.; Ono, R.; Pidcock, A. *Can. J. Chem.* **1984**, *62*, 696. (b) Capdevila, M.; Carrasco, Y.; Clegg, W.; Coxall, R. A.; González-Duarte, P.; Lledós, A.; Ramírez, J. A. *J. Chem. Soc., Dalton Trans.* **1999**, 3103.

Table 2. Selected Bond Lengths (Å) and Angles (deg)

	Complex **1a**$(ClO_4)\cdot H_2O$		
Pd(1)−Pd(2)	3.065(1)	S(1)−S(1)*	2.827(4)
Pd(2)−Pd(2)*	3.027(1)	Pd(1)−N(1)	2.045(6)
Pd(1)−S(1)	2.287(2)	Pd(2)−N(2)	2.062(7)
Pd(2)−S(1)	2.284(2)	Pd(2)−N(3)	2.049(7)
S(1)−Pd(1)−S(1)*	76.33(8)	S(1)−Pd(2)−N(3)	102.1(2)
S(1)−Pd(1)−N(1)	102.2(2)	N(1)−Pd(1)−N(1)*	79.4(3)
S(1)−Pd(1)−N(1)*	178.5(2)	N(2)−Pd(2)−N(3)	79.2(3)
S(1)−Pd(2)−S(1)*	76.49(8)	Pd(1)−S(1)−Pd(2)	85.16(8)
S(1)−Pd(2)−N(2)	178.7(2)	Pd(2)−S(1)−Pd(2)*	86.87(8)
	Complex **1b**$(ClO_4)_2\cdot H_2O$		
Pd(1)−Pd(2)	3.156(1)	Pd(3)−S(1)	2.300(2)
Pd(1)−Pd(3)	3.0749(9)	Pd(3)−S(2)	2.295(2)
Pd(2)−Pd(3)	3.095(1)	Pd(1)−N(1)	2.085(8)
Pd(1)−S(1)	2.282(3)	Pd(1)−N(2)	2.076(7)
Pd(1)−S(2)	2.302(2)	Pd(2)−N(3)	2.057(8)
Pd(2)−S(1)	2.289(2)	Pd(2)−N(4)	2.059(7)
Pd(2)−S(2)	2.278(3)	Pd(3)−N(5)	2.057(7)
		Pd(3)−N(6)	2.063(8)
S(1)−Pd(1)−S(2)	76.79(9)	S(2)−Pd(2)−N(3)	171.8(2)
S(1)−Pd(1)−N(1)	177.2(2)	S(2)−Pd(2)−N(4)	100.9(2)
S(1)−Pd(1)−N(2)	100.0(2)	N(3)−Pd(2)−N(4)	79.8(3)
S(2)−Pd(1)−N(1)	103.6(2)	Pd(1)−S(1)−Pd(2)	87.31(9)
S(2)−Pd(1)−N(2)	173.4(2)	Pd(1)−S(1)−Pd(3)	84.29(9)
N(1)−Pd(1)−N(2)	79.9(3)	Pd(2)−S(1)−Pd(3)	84.79(8)
S(1)−Pd(2)−S(2)	77.14(9)	Pd(1)−S(2)−Pd(2)	87.12(8)
S(1)−Pd(2)−N(3)	103.3(2)	Pd(1)−S(2)−Pd(3)	83.95(8)
S(1)−Pd(2)−N(4)	172.0(2)	Pd(2)−S(2)−Pd(3)	85.17(9)
	Complex **2a**$(ClO_4)_2\cdot H_2O$		
Pt(1)−Pt(2)	3.127(1)	S(1)−S(1)*	2.847(4)
Pt(2)−Pt(2)*	3.154(1)	Pt(1)−N(1)	2.034(6)
Pt(1)−S(1)	2.304(2)	Pt(2)−N(2)	2.036(7)
Pt(2)−S(1)	2.303(3)	Pt(2)−N(3)	2.039(7)
S(1)−Pt(1)−S(1)*	76.3(1)	S(1)−Pt(2)−N(3)	178.5(2)
S(1)−Pt(1)−N(1)	102.4(2)	N(1)−Pt(1)−N(1)*	78.8(4)
S(1)−Pt(1)−N(1)*	178.6(2)	N(2)−Pt(2)−N(3)	79.3(3)
S(1)−Pt(2)−S(1)*	76.4(1)	Pt(1)−S(1)−Pt(2)	85.47(8)
S(1)−Pt(2)−N(2)*	102.2(2)	Pt(2)−S(1)−Pt(2)*	86.44(8)

been offered for this phenomenon, and we suggest that crystal packing effects exert a major contribution. For diimine-supported $[M_3S_2]$ complexes, the M−S and M−N bond lengths are generally unremarkable, except that the Pd−S distances in **1a** (mean 2.286 Å) and **1b** (mean 2.291 Å) are slightly shorter than those in phosphine ($[Pd_3(PMe_3)_6(\mu_3\text{-}S)_2](BPh_4)_2$,[2b] mean 2.335 Å) and arsine ($[Pd_3(dpae)_3(\mu_3\text{-}S)_2](BPh_4)_2$,[13] mean 2.337 Å, dpae = 1,2-bis(diphenylarsino)ethane) congeners.

Absorption and Emission Spectroscopy. The UV−visible absorption data of the $[M_3S_2]$ complexes, together with that of their precursor complexes for comparison, are summarized in Table 3. The absorption spectra of the Pd(II) precursors $[Pd(^tBu_2bpy)Cl_2]$ and $[Pd((CO_2Me)_2bpy)Cl_2]$ are dominated by intraligand transitions at $\lambda < 320$ ($\epsilon_{max} = 1.6 \times 10^4$ mol^{-1} dm^3 cm^{-1}) and 340 nm ($\epsilon_{max} = 1.4 \times 10^4$ mol^{-1} dm^3 cm^{-1}), respectively. Intraligand transitions for the Pt analogues are observed in the same spectral region. The absorption shoulder at 353 nm for $[Pd((CO_2Me)_2bpy)Cl_2]$ may contain [Pd → π*$((CO_2Me)_2bpy)$] metal-to-ligand charge transfer (MLCT) character. The Pt(II) precursors $[Pt(^tBu_2bpy)Cl_2]$ and $[Pt((CO_2Me)_2bpy)Cl_2]$ exhibit an intense absorption at λ_{max} 388 (ϵ = 4500 mol^{-1} dm^3 cm^{-1}) and 423 nm (ϵ = 5200 mol^{-1} dm^3 cm^{-1}) respectively in dichloromethane. These bands are not assigned to the intraligand transition of the diimine ligands since the Pd(II) analogues absorb weakly at $\lambda > 370$ nm. In addition, a solvatochromic shift to 378 nm in acetonitrile for $[Pt(^tBu_2bpy)Cl_2]$ is observed, and hence a singlet [Pt → π*(diimine)] MLCT transition is invoked. The ^{1}MLCT transition for $Pt(bpy)Cl_2$ was previously assigned to an intense band at 394 nm in butyronitrile.[14] The observed red shift from $[Pt(^tBu_2bpy)Cl_2]$ to $[Pt((CO_2Me)_2bpy)Cl_2]$ is also in accordance with the MLCT formulation since the π* acceptor orbital of the $(CO_2Me)_2bpy$ ligand would be lower in energy due to the electronic effect of the ester groups.

The UV−vis absorption spectra for **1a** and **1b** in dichloromethane (Figure 4) contain an intense band at λ_{max} 360 (ϵ = 1.57 × 10^4 mol^{-1} dm^3 cm^{-1}) and 384 nm (ϵ = 1.61 × 10^4 mol^{-1} dm^3 cm^{-1}), respectively. Their electronic origins are proposed to be similar because of the comparable extinction coefficients. The substantial shift (∼1740 cm^{-1}) in transition energy from **1a** to **1b** indicates the involvement of the diimine ligands in the transitions, and is similar to that (∼1530 cm^{-1}) observed from ($[Pd(^tBu_2bpy)Cl_2]$ (315 nm) to $[Pd((CO_2Me)_2bpy)Cl_2]$) (331 nm). Hence these bands are unlikely to be [p(S) → Pd(II)] transitions. Reasonable candidates include [Pd → π*(diimine)] MLCT, [S(p) → π*(diimine)] ligand-to-ligand charge transfer (LLCT), and mixed [Pd(d)/S(p) → π*(diimine)] transitions. For **1b** (Figure 5), the observation that the 384 nm absorption undergoes a solvatochromic shift in acetonitrile and ethanol (374 and 377 nm, respectively) is consistent with the charge-transfer assignment described above. In concentrated solutions of **1a** and **1b**, weak shoulders are observed around 460 nm (21 500 cm^{-1}, $\epsilon \approx$ 440 mol^{-1} dm^3 cm^{-1}) and 450 nm (22 200 cm^{-1}, $\epsilon \approx$ 800 mol^{-1} dm^3 cm^{-1}), respectively, with tailing to 600 nm; these weak absorptions are tentatively assigned to d−d transitions (see below). Significantly, the lowest energy spin-allowed d−d transitions for PdX_4^{2-} occur at 21 700 and 20 200 cm^{-1} for X = Cl$^-$ and Br$^-$, respectively.[15]

Complexes **2a** and **2b** display an intense and broad absorption band in dichloromethane at λ_{max} 415 (ϵ = 2.16 × 10^4 mol^{-1} dm^3 cm^{-1}) and 448 nm (ϵ = 1.71 × 10^4 mol^{-1} dm^3 cm^{-1}) with tailing down to 500 ($\epsilon \approx$ 300 mol^{-1} dm^3 cm^{-1}) and 550 nm ($\epsilon \approx$ 500 mol^{-1} dm^3 cm^{-1}), respectively (Figure 6). These absorptions display profiles similar to those of the 388 and 423 nm bands for $[Pt(^tBu_2bpy)Cl_2]$ and $[Pt((CO_2Me)_2bpy)Cl_2]$, respectively, except that they exhibit higher ϵ_{max} values. Assignment of these bands to [p(S) → π*(diimine)] LLCT is not favored because the Pd_3 analogues do not exhibit similar absorption bands at $\lambda > 400$ nm, although sulfide-to-diimine[16a] and thiolate-to-diimine[16b] LLCT transitions have previously been assigned for absorption bands at $\lambda_{max} > 400$ nm for related Pt(II) derivatives. We tentatively assign the 415 and 448 nm bands to singlet [5d(Pt) → π*(diimine)] MLCT transitions. This is consistent with the solvatochromic behavior of this absorption band for **2a** [λ_{max} 415 (CH_2Cl_2), 405 (CH_3CN), 408 nm (CH_3CH_2OH)]. Because of the extremely low product yield for complex **2b** and the absence of structural elucidation by X-ray crystallography, a more comprehensive study on its spectroscopic properties was not pursued. Since there are three Pt centers in **2a** and **2b**, it is reasonable for the ϵ_{max} value of the MLCT band to be substantially higher than that for the $[Pt(diimine)Cl_2]$ precursors. However, it is likely that the MLCT transition is perturbed by weak Pt−Pt interactions as observed in the crystal structure of **2a** (see above). Attempts to locate

(13) Matsumoto, K.; Takahashi, K.; Hada, S.; Nakao, Y. *Polyhedron* **1999**, *18*, 1811.

(14) (a) Miskowski, V. M.; Houlding, V. H. *Inorg. Chem.* **1989**, *28*, 1529. (b) Miskowski, V. M.; Houlding, V. H.; Che, C. M.; Wang, Y. *Inorg. Chem.* **1993**, *32*, 2518.

(15) Rush, R. M.; Martin, D. S., Jr.; LeGrand, R. G. *Inorg. Chem.* **1975**, *14*, 2543.

(16) (a) Kunkely, H.; Vogler, A. *Inorg. Chim. Acta* **1997**, *264*, 305. (b) Cummings, A. D.; Eisenberg, R. *J. Am. Chem. Soc.* **1996**, *118*, 1949.

Table 3. Photophysical Data

complex	medium	*T*, K	λ^{abs}, nm (ϵ, 10^3 mol^{-1} dm^3 cm^{-1})	λ^{em}, nm (lifetime, μs)
[Pd(^{t}Bu$_2$bpy)Cl$_2$][a]	CH_2Cl_2	298	304 (13.8), 315 (16.4), 327 (sh, 3.4)	non-emissive
[Pd((CO$_2$Me)$_2$bpy)Cl$_2$][a]	CH_2Cl_2	298	324 (12.2), 331 (14.3), 353 (sh, 2.6)	non-emissive
[Pt(^{t}Bu$_2$bpy)Cl$_2$][b]	CH_2Cl_2	298	282 (28.0), 310 (8.5), 322 (9.0), 388 (4.5)	non-emissive
[Pt((CO$_2$Me)$_2$bpy)Cl$_2$][c]	CH_2Cl_2	298	302 (23.7), 325 (sh, 10.9), 340 (7.6), 423 (5.2)	non-emissive
[Pd$_3$(^{t}Bu$_2$bpy)$_3$(μ_3-S)$_2$][ClO$_4$]$_2$, **1a**(ClO$_4$)$_2$	CH_2Cl_2	298	292 (60.4), 360 (sh, 15.7), 460 (sh, 0.44)	non-emissive
	CH_3CN	298	291 (61.5), 350 (sh, 17.9), 460 (sh, 0.94)	non-emissive
	EtOH	298	291 (56.5), 360 (sh, 13.6), 460 (sh, 0.27)	non-emissive
	solid	298		730[d] (0.4)
	solid	77		760[d] (16, 51)[e]
	EtOH:MeOH	77		780[d] (35)
[Pd$_3$((CO$_2$Me)$_2$bpy)$_3$(μ_3-S)$_2$][ClO$_4$]$_2$, **1b**(ClO$_4$)$_2$	CH_2Cl_2	298	289 (59.4), 320 (48.5), 384 (16.1), 450 (sh, 0.8)	non-emissive
	CH_3CN	298	287 (58.2), 319 (46.0), 374 (15.5), 450 (sh, 1.4)	non-emissive
	EtOH	298	288 (47.7), 321 (37.9), 377 (12.8), 450 (sh, 1.2)	non-emissive
	solid	298		non-emissive
	solid	77		760[d] (22)
	EtOH:MeOH	77		780[d] (35)
[Pt$_3$(^{t}Bu$_2$bpy)$_3$(μ_3-S)$_2$[ClO$_4$]$_2$, **2a**(ClO$_4$)$_2$	CH_2Cl_2	298	303 (37.6), 317 (32.9), 415 (21.6)	non-emissive
	CH_3CN	298	303 (33.1), 317 (30.1), 405 (19.8)	non-emissive
	EtOH	298	303 (35.3), 317 (31.6), 408 (21.0)	non-emissive
	solid	298		620 (0.7, 3.7)[e]
	solid	77		630 (1.8, 7.0)[e]
	butyronitrile	77		640 (7.4)
	EtOH:MeOH	77		645 (7.1)
[Pt$_3$((CO$_2$Me)$_2$bpy)$_3$(μ_3-S)$_2$][ClO$_4$]$_2$, **2b**(ClO$_4$)$_2$	CH_2Cl_2	298	309 (33.7), 334 (sh, 22.6), 448 (17.1)	non-emissive
	solid	298		610 (0.25)
	solid	77		618 (10.2)
[Pt$_3$(dppm)$_3$(μ_3-S)$_2$][ClO$_4$]$_2$, **3**(ClO$_4$)$_2$	CH_2Cl_2	298	264 (68.3), 284 (sh, 49.5)	non-emissive
	solid	298		593 (1.4)
	solid	77		616 (19)
	EtOH:MeOH	77		597 (24)

[a] Non-emissive in the solid state. [b] Solid-state emissions at 632 (77 K) and 645 nm (10 K, data from ref 17). [c] Solid-state emissions at 658 (298 K) and 664 nm (77 K). [d] Uncorrected; errors may be present due to instrumental limitation. [e] Biexponential decay.

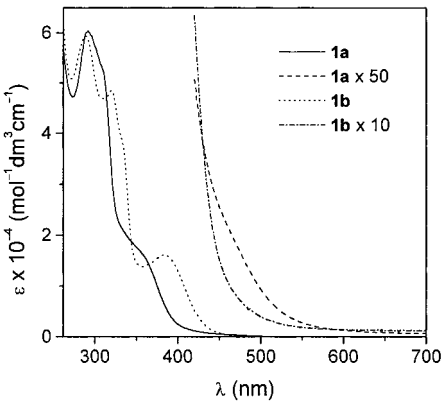

Figure 4. UV−visible absorption spectra of **1a** and **1b** in dichloromethane.

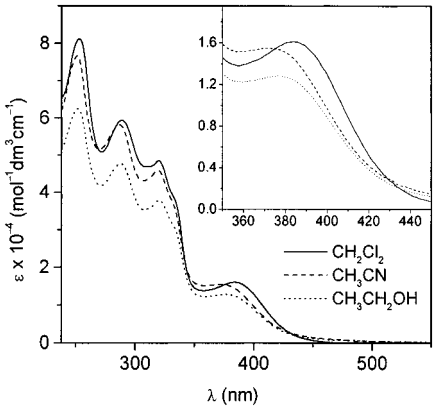

Figure 5. UV−visible absorption spectra of **1b** in various solvents.

weak ^{3}MLCT and/or d−d transitions at wavelengths above 450 nm were unsuccessful, even at concentrations of $\sim 10^{-3}$ mol dm^{-3} in CH_2Cl_2. Complex **3** absorbs in the UV region at λ_{max} 264 nm ($\epsilon = 6.8 \times 10^4$ mol^{-1} dm^3 cm^{-1}) with a shoulder at 284 nm and tailing down to 400 nm in dichloromethane (see Supporting Information). There is no distinct absorption band at wavelengths greater than 350 nm.

All [M_3S_2] complexes are non-emissive in solution at room temperature. At 298 K, the Pt(II) derivatives **2a**, **2b**, and **3** display unstructured solid-state emission at λ_{max} 620, 610, and 593 nm, respectively (full width at half-maximum, fwhm = 3590, 2500, and 4560 cm^{-1}, respectively; inset in Figure 6 shows 298 K solid-state emission of **2a**). At 77 K, an increase in the emission intensity is accompanied by a slight red shift to λ_{max} 630, 618, and 616 nm for **2a**, **2b**, and **3** (see Supporting Information), respectively, but no vibronic fine structure is detected. In a 77 K ethanol/methanol glass, the emission maximum of **2a** red-shifts to 645 nm and a strong match between the corresponding excitation spectrum and the solution absorption is observed. An alcoholic glassy solution of **3** emits at 597 nm, again with close resemblance between the excitation and absorption spectra.

The Pd_3 derivative **1a** weakly emits at λ_{max} 730 nm (uncorrected) in the solid state at room temperature. Both **1a** and **1b** solids exhibit comparable 77 K emissions at λ_{max} 760 nm, and the excitation spectrum of **1a** (Figure 7) depicts the absorption edge at $\sim$493 nm with tailing down to 600 nm (cf. weak absorption band at 460 nm in Figure 4). A more intense and red-shifted emission is evident in 77 K alcoholic glasses (uncorrected λ_{max} 780 nm) for **1a** and **1b**, and the corresponding excitation also closely resembles its solution absorption.

We tentatively assign these emissions to excited states that are ligand-field in nature. The absence of photoluminescence for [M_3S_2] complexes in fluid solution at room temperature implies that the emissive excited states undergo significant

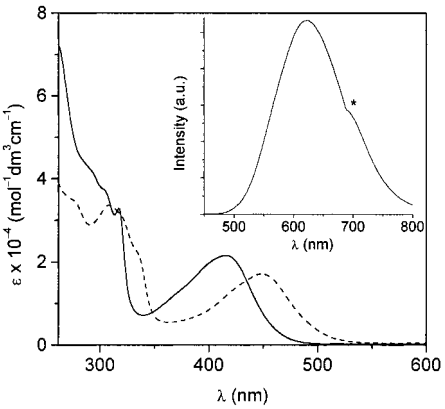

Figure 6. UV−visible absorption spectra of **2a** (—) and **2b** (---) in dichloromethane (Inset: 298 K solid-state emission spectrum of **2a**; * denotes instrumental artifact).

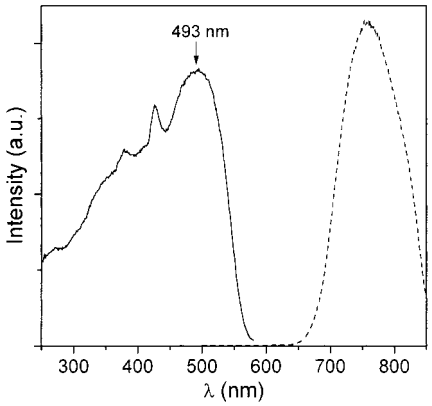

Figure 7. 77 K solid-state emission (---) and excitation (—) spectra of **1a** (uncorrected).

structural distortions from the ground state, leading to facile non-radiative decay pathways. The emission of phosphine-supported platinum(II) derivative **3** at ∼600 nm is unlikely to originate from [d(Pt) → π*(phosphine)] MLCT or [π(S) → π*(phosphine)] LLCT excited states as the emission energy is incompatible with the π* orbital of the dppm ligand. Assignment of the phosphorescence of **3** to a ligand-field excited state is in good agreement with the large Stoke shift from the lowest energy allowed transition at 284 nm (∼18 500 cm^{-1}), bandwidth (3020 cm^{-1}), and long excited-state lifetime (24 μs) in 77 K alcoholic glass. Furthermore, the 77 K glassy emissions for $Pt(bpy)Cl_2$ (methanol: λ_{max} 610 nm, fwhm ∼3600 cm^{-1}; butyronitrile: λ_{max} 625 nm) and related α-diimine derivatives have been proposed to originate from ligand-field excited states.[15] Because of the resemblance between the luminescence of **2a** with **3** and $Pt(bpy)Cl_2$ (in emission energies and bandwidths), plus the large Stokes shift of ∼9000 cm^{-1} from the ^{1}MLCT transition in ethanol (408 nm) and the lack of vibronic structure for **2a**, a ^{3}d−d excited state is indicated. For **2b**, introduction of ester substituents on the diimine ligand does not significantly change the emission energies. The solid-state emission of **2b** is thus cautiously assigned to a ligand-field excited state. However, due to the electron-withdrawing effect of the CO_2Me groups, the ^{3}MLCT and ^{3}d−d transitions may occur at similar energies.[14b] Hence, an excited state with admixture of ^{3}d−d and ^{3}MLCT character cannot be excluded.[17]

The solid-state luminescence of the $[Pd_3S_2]$ complexes **1a** and **1b** are assigned as ^{3}d−d in nature. Both the absorption and solid-state/glassy excitation spectra for **1a** and **1b** reveal the presence of low-energy ligand-field states in the 460−600 nm spectral region. Moreover, changes in the electronic nature of the substituent on the diimine ligand (*tert*-butyl, ester) clearly does not alter the emissive properties of the $[Pd_3S_2]$ species **1a** and **1b**. This signifies that the emission originates from a metal-centered ^{3}d−d excited state. Finally, the red shifts for the emission energies from $[Pt_3S_2]$ to $[Pd_3S_2]$ are entirely consistent with the observation that the d−d excited states of Pd(II) are lower in energy compared to Pt(II).[18]

Acknowledgment. We are grateful for financial support from The University of Hong Kong, the Croucher Foundation of Hong Kong, and the Research Grants Council of the Hong Kong SAR, China [HKU 7298/99P]. We thank Dr. N. Zhu for the structural determination of complex **3**$(ClO_4)_2$, Dr. V. M. Miskowski for helpful discussions, Dr. W. F. Fu for some of the spectroscopic measurements, and the reviewers for valuable comments and suggestions.

Supporting Information Available: UV−visible absorption and 77 K solid-state emission spectra of **3**$(ClO_4)_2$; listings of crystal data, atomic coordinates, calculated coordinates, anisotropic displacement parameters, and bond lengths and angles for **1a**$(ClO_4)_2 \cdot H_2O$, **1b**$(ClO_4)_2 \cdot H_2O$, **2a**$(ClO_4)_2 \cdot H_2O$, and **3**$(ClO_4)_2$. This material is available free of charge via the Internet at http://pubs.acs.org.

IC010891R

(17) Houlding, V. H.; Miskowski, V. M. *Coord. Chem. Rev.* **1991**, *111*, 145.
(18) Mason, W. R.; Gray, H. B. *J. Am. Chem. Soc.* **1968**, *90*, 5721.